Heterogeneity of firing properties among rat thalamic reticular nucleus neurons

Sang-Hun Lee, G. Govindaiah and Charles L. Cox

Department of Molecular & Integrative Physiology, Department of Pharmacology and Beckman Institute, University of Illinois, Urbana, IL 61801, USA

The thalamic reticular nucleus (TRN) provides inhibitory innervation to most thalamic relay nuclei and receives excitatory innervation from both cortical and thalamic neurons. Ultimately, information transfer through the thalamus to the neocortex is strongly influenced by TRN. In addition, the reciprocal synaptic connectivity between TRN with associated thalamic relay nuclei is critical in generating intrathalamic rhythmic activities that occur during certain arousal states and pathophysiological conditions. Despite evidence suggesting morphological heterogeneity amongst TRN neurons, the heterogeneity of intrinsic properties of TRN neurons has not been systematically examined. One key characteristic of virtually all thalamic neurons is the ability to produce action potentials in two distinct modes: burst and tonic. In this study, we have examined the prevalence of burst discharge within TRN neurons. Our intracellular recordings revealed that TRN neurons can be differentiated by their action potential discharge modes. The majority of neurons in the dorsal TRN (56%) lack burst discharge, and the remaining neurons (35%) show an atypical burst that consists of an initial action potential followed by small amplitude, long duration depolarizations. In contrast, most neurons in ventral TRN (82%) display a stereotypical burst discharge consisting of a transient, high frequency discharge of multiple action potentials. TRN neurons that lack burst discharge typically did not produce low threshold calcium spikes or produced a significantly reduced transient depolarization. Our findings clearly indicate that TRN neurons can be differentiated by differences in their spike discharge properties and these subtypes are not uniformly distributed within TRN. The functional consequences of such intrinsic differences may play an important role in modality-specific thalamocortical information transfer as well as overall circuit level activities.

(Resubmitted 10 April 2007; accepted after revision 23 April 2007; first published online 26 April 2007)
Corresponding author C.L. Cox: Department of Molecular and Integrative Physiology, 2357 Beckman Institute, 405 North Mathews Avenue, Urbana, IL 61801, USA. Email: cox2@uiuc.edu

The thalamic reticular nucleus (TRN) is a thin shell of GABA-containing neurons surrounding the anterolateral regions of the dorsal thalamus providing synaptic innervation of underlying thalamic relay nuclei. TRN neurons receive synaptic input from collaterals of thalamocortical and corticothalamic neurons, and thus these cells are in a unique position to provide feed-back inhibition to thalamic relay nuclei from thalamocortical neurons and feed-forward inhibition by way of cortico-thalamic neurons. The inhibitory influence on relay neurons can regulate the transfer of sensory information from the dorsal thalamus to the neocortex as demonstrated by changes in receptive fields of dorsal thalamic neurons following manipulation of TRN neuronal activity (Hale *et al.* 1982; Ahlsén *et al.* 1985; Shosaku *et al.* 1989; Lee *et al.* 1994). In addition, as a result of the reciprocal synaptic relationship between TRN and thalamic relay nuclei, TRN neurons play a critical role in intrathalamic rhythmic activities similar to those observed during various sleep states and absence epilepsy (Steriade *et al.* 1993; von Krosigk *et al.* 1993; Warren *et al.* 1994; Huguenard & Prince, 1994; Cox *et al.* 1997*b*; Lee & Cox, 2006). In addition, it appears that TRN may serve to relay information between first-order (primary sensory) thalamic nuclei and higher-order thalamic nuclei (Crabtree *et al.* 1998; Crabtree, 1999; Crabtree & Isaac, 2002). Thus, TRN appears to play several critical roles in thalamocortical circuit function, and a clear understanding of intrinsic properties of these cells may allow a better understanding of their functional role.

With regards to intrinsic properties, TRN neurons have long been considered a relatively homogeneous population of GABA-containing neurons that provide diffuse inhibitory influence on thalamocortical neurons. Several studies have differentiated TRN neuron subtypes based solely upon morphological criteria including soma size, soma shape, dendritic architecture, and axonal arbor morphology (Scheibel & Scheibel, 1966; Jones, 1975;

 DOI: 10.1113/jphysiol.2007.134254

Houser *et al.* 1980; Yen *et al.* 1985; Domich *et al.* 1986; Spreafico *et al.* 1988; Avanzini *et al.* 1989; Spreafico *et al.* 1991; Contreras *et al.* 1993; Cox *et al.* 1996). Despite anatomical evidence supportive of multiple TRN neuron subtypes, the functional significance of these distinct subpopulations is rather limited (Cox *et al.* 1997*a*). One common characteristic of virtually all thalamic neurons including TRN neurons is the presence of two distinct modes of action potential discharge: burst and tonic modes (Domich *et al.* 1986; Mulle *et al.* 1986; Steriade *et al.* 1986; Spreafico *et al.* 1988). Burst mode is characterized by a transient high-frequency action potential discharge that is dependent on activation of transient, low threshold voltage-dependent Ca^{2+} channels. This firing mode appears critical for the maintenance of intrathalamic rhythms and may serve unique functions in information processing (Glenn & Steriade, 1982; Jahnsen & Llinás, 1984*a*; Coulter *et al.* 1989; Steriade *et al.* 1993; von Krosigk *et al.* 1993; Lisman, 1997; Sherman & Guillery, 2002). Although limited observations suggest that some TRN neurons do not produce burst discharge, these studies have not systematically addressed this issue (Contreras *et al.* 1992; Brunton & Charpak, 1997).

The TRN is topographically organized by modality, and thereby is subdivided into several sectors based on efferent and afferent connections to modality specific thalamic and neocortical regions. In general, ventral, anterolateral, dorsocaudal, and ventrocaudal TRN are loosely associated with somatosensory, motor, visual and auditory modalities, respectively, on the basis of the anatomical and physiological data (Jones, 1975; Hale *et al.* 1982; French *et al.* 1985; Shosaku *et al.* 1989; Conley & Diamond, 1990; Crabtree, 1992, 1996; Bourassa *et al.* 1995; Pinault *et al.* 1995*a*; Coleman & Mitrofanis, 1996; Crabtree *et al.* 1998). In the present study, we found three distinct TRN neuron subtypes based on their action potential discharge properties: non-burst, atypical burst and typical burst neurons. Furthermore, these different TRN neuron subtypes are not homogeneously distributed within TRN. In dorsal TRN regions, virtually all neurons were non-burst or atypical burst neurons. In contrast, the overwhelming majority of neurons in the ventral TRN region produce typical burst discharge (typical burst). While the functional role of non-burst neurons remains speculative, the dorsal TRN is generally associated with visually related modality, so these unique non-burst neurons may have important function in visual information processing. Some of these findings have been presented in abstract form (Lee *et al.* 2004).

Methods

Thalamic slice preparation

The procedures used in these experiments were similar to those previously described (Lee & Cox, 2003). Young Sprague–Dawley rats (postnatal age 10–28 days) were deeply anaesthetized with sodium pentobarbital (50 mg kg^{-1}, I.P. injection) and decapitated. All procedures closely followed guidelines put forth by the Department of Animal Resources at the University of Illinois. The brain was quickly removed and placed into cold, oxygenated slicing medium containing (mM): 2.5 KCl, 10.0 $MgCl_2$, 0.5 $CaCl_2$, 1.25 NaH_2PO_4, 26.0 $NaHCO_3$, 11.0 glucose, and 234.0 sucrose. Serial horizontal brain slices (300 μm thickness) were cut using a vibrating tissue slicer and collected from dorsal to ventral regions of TRN: the 1st and 2nd slices from the dorsal extent of TRN are referred to as dorsal TRN slices (dTRN). The 3rd and 4th slices are referred to as ventral TRN slices (vTRN). The 1st to 4th slices roughly correspond to Bregma −4.74, −5.10, −5.32 and −5.60, respectively (Fig. 1; Paxinos & Watson, 1986). The posterior commissure, fasciculus retroflexus and dLGN were used to distinguish the level of each slice. The fasciculus retroflexus appears in the 2nd slice as a large diameter structure, but appears as a relatively diffuse myelinated tract with a smaller diameter in the 3rd and 4th slices. The posterior commissure clearly crosses the midline in the 1st and 2nd slices, but appears interrupted in the 3rd and 4th slices (e.g. Fig. 1).

Thalamic slices were transferred to a holding chamber, and incubated at least 1 h before recording. Individual slices were then transferred to a recording chamber, and continuously superfused with oxygenated physiological saline at 30°C. The physiological solution contained (mM): 126.0 NaCl, 2.5 KCl, 2.0 $MgCl_2$, 2.0 $CaCl_2$, 1.25 NaH_2PO_4, 26.0 $NaHCO_3$, and 10.0 glucose. This solution was gassed with 95% O_2–5% CO_2 to a final pH of 7.4. In experiments using 4-aminopyridine (4-AP), the physiological solution contained (mM): 126.0 NaCl, 2.5 KCl, 2.0 $MgCl_2$, 2.0 $CaCl_2$, 10.0 Hepes, and 10.0 glucose. This solution was gassed with 100% O_2. All chemical used in this study were purchased from Sigma (St Louis, MO, USA).

Intracellular recording procedures

Intracellular recordings, using the whole-cell configuration were obtained with the visual aid of a modified Nikon microscope equipped with differential interference contrast optics. For intracellular recordings, individual slices were transferred to a submersion-type recording chamber. A low power objective (×4) was used to identify the level of each slice as well as the TRN, and a high-power water immersion objective (×40) was used to visualize individual TRN neurons. Recording pipettes were pulled from 1.5 mm outer diameter capillary tubing and had tip resistances of 3–6 MΩ when filled with the following intracellular solution containing (mM): 117.0 potassium gluconate, 13.0 KCl, 1.0 $MgCl_2$, 0.07 $CaCl_2$, 0.1 EGTA, 10.0 Hepes, 2.0 Na_2-ATP, 0.4 Na-GTP, and

0.3% biocytin. The pH was adjusted to 7.3 and osmolarity was adjusted to 290–300 mosmol l^{-1}. The initial access resistances ranged from 7 to 20 MΩ and remained stable in recordings included for analyses in this study. An Axoclamp2B or Multiclamp 700A amplifier (Molecular Devices, Sunnyvale, CA, USA) was used in bridge mode for voltage recordings or discontinuous single electrode voltage clamp mode for current recordings (Axoclamp 2A). Current and voltage protocols were generated using pCLAMP software (Molecular Devices) and data were stored on computer. For current-clamp recordings, an active bridge circuit was continuously monitored and adjusted to balance the drop in potential produced by passing current through the recording electrode. For voltage clamp recordings, the amplifier was used in discontinuous mode. In these recordings, the switching frequency ranged from 2.5 to 3.5 kHz with a gain of 150–300 pA mV^{-1}, and the headstage was continually monitored to ensure that the current transients had completely decayed before voltage measurements.

Histological procedures

Biocytin was included in the recording pipette in order to reconstruct the morphology of recorded neurons. After recording, slices were fixed overnight in 4% paraformaldehyde in 0.1 M phosphate buffer (pH 7.4). Slices were then reacted with avidin–biotin–peroxidase complex (ABC Elite, Vector Laboratories, CA, USA) using established procedures in our laboratory (Horikawa &

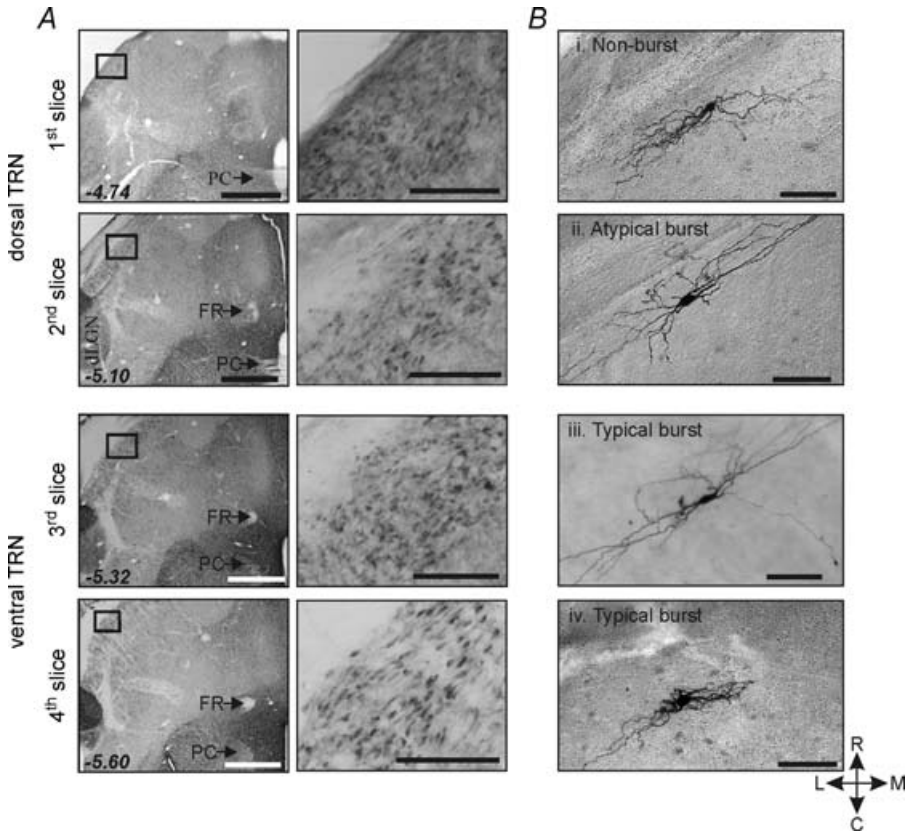

Figure 1. Localization of GAD immunoreactive neurons within TRN
A, the dorsal to ventral horizontal brain slices (1st slice to 4th slice) are shown to have the GAD immunoreactivity in the TRN indicating the 1st slice that includes the extreme dorsal portion of TRN to the 4th slice include the GABAergic TRN neurons. With lower power objective, the posterior commissure (PC) and fasciculus retroflexus (FR) are used to distinguish the level of each slice. The 1st to 4th slices correspond to −4.74, −5.10, −5.32 and −5.60 mm bregma (Paxinos & Watson, 1986). Scale bars refer to 1 mm and 200 μM. Each rectangle (left) is shown at higher power (right) to illustrate GABA-positive neurons in TRN. *B*, photomicrographs of different TRN neurons based on their burst discharge characteristics. Four TRN neurons (*i–iv*) were localized in the 1st to 4th slices. Non-burst neuron (*i*), atypical burst neuron (*ii*), and typical burst neuron (*iii*) have similar morphological characteristics. They have fusiform somas and several primary dendrites that extend from each pole of the cell body and are orientated to the longitudinal axis of the TRN. However, a subpopulation of all three subtype TRN neurons also has somewhat round-shaped soma with multipolar dendrites (*iv*), suggesting morphological diversity within each subtype. Scale bar, 100 μM. C, caudal; R, rostral; M, medial; L, lateral.

Armstrong, 1988; Govindaiah & Cox 2004). Subsequently, slices were mounted and the neurons were examined using a light microscope.

The distribution of individual neurons within the TRN (cf. Fig. 2*B*) was constructed from the relative location of the neuron within TRN relative to the borders of the nucleus. When cutting the slices used for the electrophysiological recordings, we carefully noted the relative size and shape of specific landmarks (see above: habenula, posterior commissure, fasiculus retroflexus) for consistency of slices across animals. The cells dorsal/ventral location within a given slice was accomplished by noting the depth of the cell from the surface using the DIC optics and the side of the slice from which the recording was being obtained.

For glutamic acid decarboxylase (GAD) immunohistochemistry, Sprague–Dawley rats (postnatal age 15–19 days) were deeply anaesthetized with sodium pentobarbital (60 mg kg^{-1}) and transcardially perfused with phosphate-buffered saline (PBS, pH 7.2) followed by 4% paraformaldehyde–0.5% gluteraldehyde in 0.1 M phosphate buffer (pH 7.4). Brains were removed and post-fixed overnight in paraformaldehyde. Brains were then cryoprotected in a 30% sucrose in PBS and sectioned using a cryostat (50 μm sections). Free-floating sections were processed for GAD immunohistochemistry using GAD65 mouse monoclonal anti-GAD antibody (Developmental Studies Hybridoma Bank, University of Iowa). The sections were washed in PBS (3 × 10 min), and incubated in 0.5% H_2O_2 (0.1% sodium azide) PBS for 30 min. After repeated washes in PBS (3 × 5 min), sections were incubated in 5% normal horse serum (NHS; Sigma) for 60 min, then in anti-GAD antibody (1 : 50 in 1% NHS) for 2 h at room temperature and overnight at 4°C. After PBS rinses (3 × 10 min), sections were incubated in the secondary antibody (peroxidase conjugated horse anti-mouse IgG, 1 : 100, Vector Laboratories) for 1 h. After four washes in 0.1 M PBS, sections were reacted with 0.05% diaminobenzidine, 0.002% H_2O_2 and 0.1% nickel ammonium sulphate in 0.1 M PBS, then washed and mounted on gelatin-coated slides, dehydrated and coverslipped using permount mounting medium.

Data analyses

The apparent input resistances of the neurons were calculated from the linear slope of the voltage–current relationship obtained by applying constant current pulses ranging from −100 to +40 pA (800 ms duration). The firing properties of each TRN neuron were examined at holding potentials near rest (−60 mV) and at relatively hyperpolarized membrane potential (approximately −80 mV) by applying depolarizing step currents (1 s duration; 10–40 pA increments; 15 steps). Smaller increment current steps (10–20 pA) were used in the neurons having relatively high input resistances, whereas larger increments (30–40 pA) were used in neurons having relatively lower input resistances. The amplitude of the low threshold spike (LTS) was calculated as the difference of the peak amplitude of the transient depolarization and the sustained tail amplitude of the ohmic step. In order to test for the presence of the low threshold transient calcium current (I_T), neurons were recorded using voltage clamp techniques with a holding potential of −50 mV. Command voltages from −50 to −125 mV (5 mV increments, 16 steps, 1 s duration) were subsequently applied and then stepped back to the holding potential (−50 mV) in order to evoke the transient inward current. The quantification of action potential characteristics was made using pCLAMP software (Molecular Devices, Inc.). Action potential amplitudes were calculated as from baseline to peak, and half-width durations were calculated as the duration of the response at 50% maximum amplitude. All data are presented as the mean ± standard deviation. Statistical analyses usually consisted of the Mann–Whitney *U* test, and when appropriate, one-way analysis of variance (ANOVA) with the Tukey–Kramer multiple comparisons test. The difference between means was considered significant when $P < 0.05$.

Results

Diversity of firing modes of TRN neurons

Current dogma is that a ubiquitous characteristic of thalamic neurons, including TRN neurons, is the ability to produce burst discharge of action potentials. In this study, we systematically examined the action potential discharge properties of TRN neurons relative to their distribution within TRN. Intracellular recordings were obtained from a total of 211 TRN neurons and these cells were subdivided by their action potential discharge characteristics. Of these neurons 170 biocytin-containing cells were recovered and then mapped as to their localization within TRN. To confirm that all four thalamic slices (dorsal to ventral slices, see Methods) do indeed contain TRN, GAD-immunohistochemistry was performed to localize GABA-positive regions within each of the four slices (Fig. 1*A*). As expected, GAD-immunoreactive neurons were found in all levels of TRN slices, further supporting that electrophysiological recordings obtained in this study were indeed restricted to TRN. Furthermore, all neurons recorded were found within the boundaries of TRN and the morphology of these neurons is consistent with previous findings that most TRN neurons have fusiform-shaped somata with either bipolar or multipolar primary dendrites (Fig. 1*B*; Spreafico *et al.* 1988; Cox *et al.* 1996).

Surprisingly, the majority of TRN neurons (56%: 71/127) obtained from dTRN (1st and 2nd slices) did not produce burst discharge even from relatively hyperpolarized membrane potentials of −80 mV (Fig. 2*Aa*, Non-burst). In a smaller population of dTRN neurons (35%: 44/127), the apparent burst discharge consisted of an initial action potential followed by multiple small amplitude, long duration depolarizing potentials (Fig. 2*Aa*, Atypical burst). Only a minor population of neurons in dTRN (9%: 12/127) produced a stereotypical burst discharge consisting of high frequency, multiple large amplitude action potentials similar to that previously described in TRN and other thalamic neurons (Fig. 2*Aa*, Typical burst). Considering the

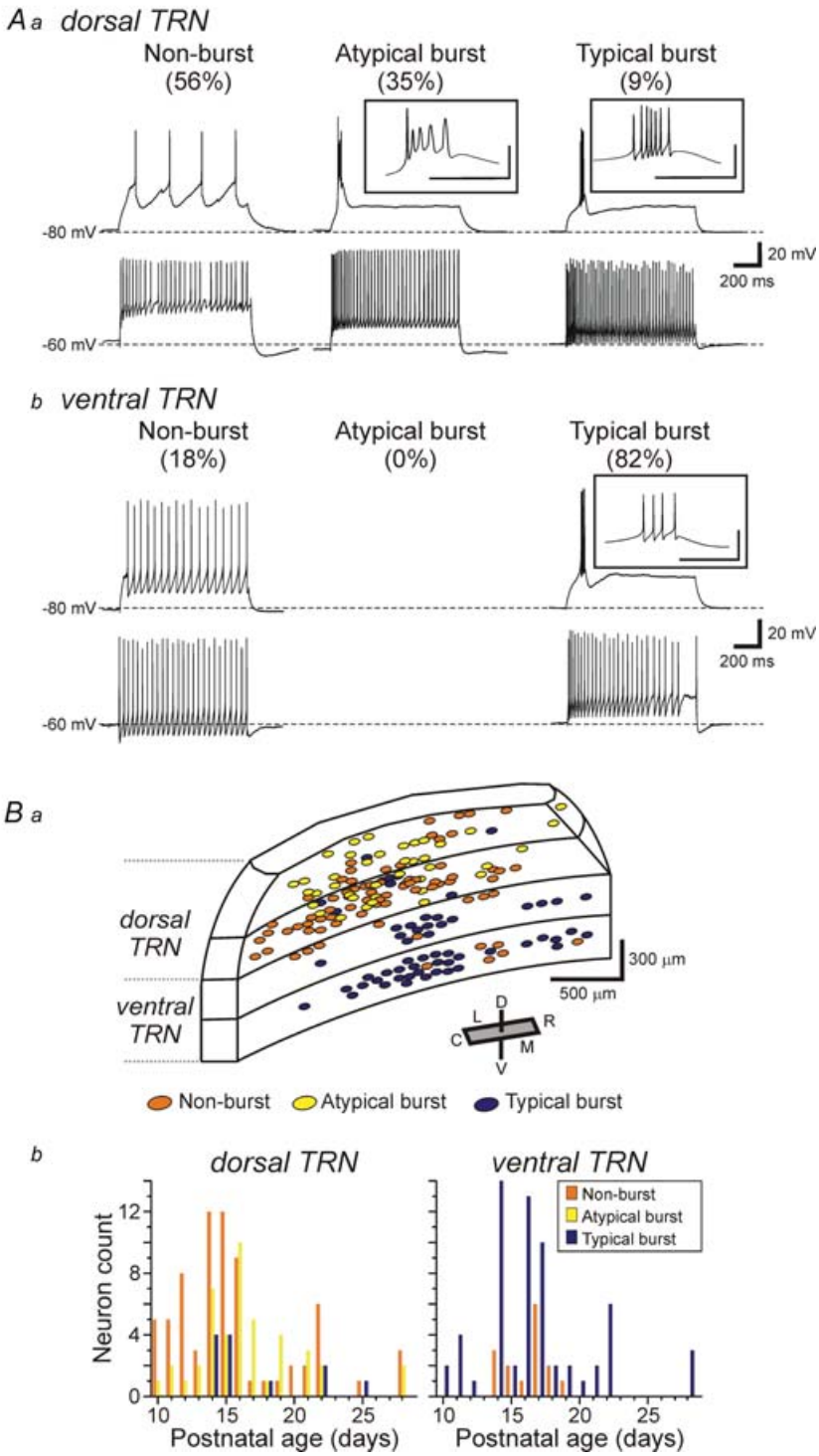

Figure 2. Distinct firing modes of TRN neurons and their distribution within TRN
Aa, in dorsal TRN, current clamp recordings illustrate three different subtypes of TRN neurons based on their ability to produce burst discharge: non-burst (left), atypical burst (middle), and typical burst (right). The neurons were manually hyperpolarized to membrane potentials of −80 mV, and then depolarizing current steps were used to evoke action potential discharge. Non-burst neurons responded to the current step with tonic action potential discharge. Atypical burst neurons characteristically had an initial normal action potential followed by depolarizing potentials with smaller amplitude and longer duration than a typical action potential. Typical burst neurons produced a high frequency, transient action potential discharge in response to the current step. At a depolarized holding potential (−60 mV), all three neuron subtypes produced tonic action potential discharge in response to a depolarizing current pulse. *b*, in ventral TRN, current clamp recordings illustrate two different subtypes of TRN neurons; non-burst (left) and typical burst (right) at different holding potentials. Insets illustrate the initial action potential discharge on a faster time base. Inset scale: 40 mV, 50 ms. *B*, distribution of the three neuronal subtypes within the TRN. *a*, non-burst and atypical burst neurons are almost exclusively localized within the dorsal TRN slices (1st and 2nd slices). In contrast, almost all neurons in the ventral TRN slices (3rd and 4th slices) respond with stereotypical burst discharge. Note that non-burst neurons in the 3rd slice were located on the dorsal side of the slice. Abbreviations: D, dorsal; V, ventral; C, caudal; R, rostral; L, lateral; M, medial. *b*, distribution of the three TRN neuron subtypes as a function of age. Note that all three subtypes are observed across the range of ages tested.

Table 1. Intrinsic properties and action potential (AP) characteristics of TRN neurons

	Intrinsic properties		Action potential characteristics					
			Amplitude			Half-width	Frequency	
	Membrane potential (mV)	Input resistance (mΩ)	1st AP (mV)	2nd AP (mV)	3rd AP (mV)	1st AP (ms)	1st interval (Hz)	2nd Interval (Hz)
Atypical Burst	-69.9 ± 4.7 ($n = 30$)	330 ± 76 ($n = 30$)	92.5 ± 8.6 ($n = 23$)	65.5 ± 8.0 ($n = 23$)	70.3 ± 7.0 ($n = 15$)	1.29 ± 0.30 ($n = 21$)	226.2 ± 48.3 ($n = 23$)	140.8 ± 39.7 ($n = 15$)
Typical Burst	-70.0 ± 6.8 ($n = 61$)	226 ± 87 ($n = 62$)	88.9 ± 8.2 ($n = 22$)	88.2 ± 7.6 ($n = 22$)	83.7 ± 7.5 ($n = 15$)	0.69 ± 0.23 ($n = 22$)	124.7 ± 46.9 ($n = 22$)	171.5 ± 65.0 ($n = 15$)
Non-burst	-66.5 ± 8.0 ($n = 46$)	421 ± 184 ($n = 60$)	92.6 ± 9.3 ($n = 22$)			1.37 ± 0.72 ($n = 22$)		
	$P < 0.001$ ANOVA	$P < 0.001$ ANOVA	n.s. ANOVA	$P < 0.01$ *t* test	$P < 0.01$ *t* test	$P < 0.001$ ANOVA	$P < 0.01$ *t* test	n.s. *t* test

*These analyses was limited to neurons obtained in slices from P15 to P19 animals. The *n* values represent number of cells tested. Abbreviations: n.s., not significant.

apparent difference in the transient discharge by the typical burst and atypical burst neurons, we quantified three different characteristics of action potentials in these cells. Namely, we measured the amplitudes of the first three action potentials, the half-width of the first action potential, and the instantaneous firing frequency of the first two action potential intervals (Table 1). The amplitude of the 1st action potential in the burst did not differ between atypical burst and typical burst neurons ($P > 0.2$, one-way ANOVA with Tukey–Kramer multiple comparisons test); however, the subsequent two action potentials were significantly smaller in the atypical burst neurons ($P < 0.01$, *t* test). The half-width of the initial action potential was also significantly shorter in the typical burst neurons compared to the atypical burst and non-burst neurons (Tables 1, $P < 0.001$, one-way ANOVA with Tukey–Kramer multiple comparisons test). Throughout this study, long duration current pulses (1 s duration) were used to evoke action potential discharge; however, in many studies, shorter duration current steps are used to produce burst discharge. In a subpopulation of neurons, shorter current steps (30–50 ms) were used to evoke burst discharge in order to assure that the differences that we observed in the discharge properties of the TRN neurons were not a result of the longer current steps. As illustrated in Fig. 3*A*, the duration of current pulses (50 ms *versus* 1 s) did not alter the discharge properties of the different TRN neuron subtypes ($n = 5$ for each TRN neuron subtype).

As expected, when the membrane potential was held at a relatively depolarized level (> -60 mV), all TRN neurons produced tonic action potential discharge indicating the voltage dependence of the burst discharge, when present (Fig. 2*Aa*). In contrast to dTRN, the majority of neurons recorded from vTRN slices (3rd and 4th slices) displayed typical burst discharge (82%: 69/84, Fig. 2*Ab*, Typical burst). The remaining 18% (15/84) of the neurons in vTRN slices were non-burst neurons (Fig. 2*Ab*, Non-burst); however, it is interesting to note that seven of these cells were located near the dorsal surface of the 3rd slices, further supporting that non-burst neurons are preferentially localized in dTRN (Fig. 2*Ba*, orange circles). It is important to note that we found all three TRN subtypes in slices from older animals as well (up to postnatal age 28 days, Fig. 2*Bb*), suggesting that the atypical and non-burst neurons are not simply an immature state of typical burst neurons.

As illustrated in Fig. 2*Ba*, the distribution of 170 TRN neurons has been mapped: 73 non-burst, 40 atypical burst, and 57 typical burst neurons. The non-burst and atypical burst neurons were almost exclusively localized within the dTRN (slices 1 and 2: Fig. 2*Ba*).These neurons do not appear to be differentially distributed across the anterior/posterior extent of TRN. In contrast, the vast majority of vTRN neurons showed stereotypical burst discharge (Fig. 2*Ba*, Typical burst, blue circles). Considering TRN neurons have been differentiated by soma shape and polarity within TRN (Spreafico *et al.* 1991), we also investigated whether these three TRN neuron subtypes may be differentiated by their morphology. The morphology of biocytin-filled neurons was obtained for 73 TRN neurons: 32 non-burst, 16 atypical burst, and 25 typical burst neurons (e.g. Fig. 1*B*). In these neurons the soma and dendritic arborizations were well-labelled for further analyses. We analysed the soma area, soma shape (ratio of the major and minor axis), and number of primary dendrites (Table 2). Although these basic morphological characteristics varied within each group distinguished by discharge mode, there were no significant differences in any of these morphological characteristics amongst the three groups ($P > 0.1$, one-way ANOVA). Thus, the size or shape of TRN neurons was not a prediction as to whether the neuron could produce burst discharge of action potentials.

Table 2. Morphological properties of TRN neurons

	Soma area (μm^2)	Soma shape (minor/major axis)	No. primary dendrites
Non-burst	251 ± 83 ($n = 32$)	0.55 ± 0.10 ($n = 32$)	3.3 ± 1.2 ($n = 32$)
Atypical Burst	249 ± 76 ($n = 16$)	0.53 ± 0.10 ($n = 16$)	4.0 ± 1.0 ($n = 16$)
Typical Burst	302 ± 107 ($n = 25$)	0.56 ± 0.14 ($n = 25$)	3.7 ± 1.4 ($n = 25$)

Heterogeneous membrane properties among TRN neurons

We next tested if the passive intrinsic membrane properties differed amongst these three TRN neuron subtypes (Table 1). The resting membrane potential significantly differed between burst and non-burst neuronal subtypes ($F_{2,134} = 3.9$, $P < 0.001$, one-way ANOVA). The average membrane potential of non-burst neurons (-66.5 ± 8.0 mV, $n = 46$) significantly differed from the typical burst neurons (-70.0 ± 6.8 mV, $n = 61$, $P < 0.01$, Tukey–Kramer multiple comparison test) but did not significantly differ from atypical burst neurons (-69.9 ± 4.7 mV, $n = 30$, $P > 0.1$). The apparent input resistances of neurons also significantly varied across the three neuronal populations ($F_{2,149} = 32.8$, $P < 0.01$, one-way ANOVA). Non-burst neurons had an average input resistance of 421 ± 184 MΩ ($n = 60$) which was significantly different from atypical burst neurons (330 ± 76 MΩ, $n = 30$) and typical burst neurons (226 ± 87 MΩ, $n = 62$, $P < 0.01$, Tukey–Kramer multiple comparison test). Furthermore, the input resistance of atypical burst neurons was significantly higher than that of typical burst neurons ($P < 0.01$, Tukey–Kramer multiple comparison test).

Non-burst TRN neurons lack low threshold Ca^{2+} current

Burst firing mode of thalamic neurons requires activation of the low threshold, transient Ca^{2+} current, I_T (Deschênes *et al.* 1982; Jahnsen & Llinás, 1984*b*; Coulter *et al.* 1989). Considering the dependence of I_T activation for burst discharge, we speculate that non-burst neurons may in fact lack I_T. Alternatively, I_T may be masked or inhibited by other voltage-dependent conductances such as the transient K^+ current, I_A. We initially examined whether a low threshold, transient calcium-dependent depolarization (low threshold spike: LTS) could be evoked in these different TRN neuron subtypes. From an initial membrane potential of -80 mV, depolarizing current steps (1 s duration; 10–40 pA increments; 15 steps) were applied in normal ACSF and TTX. In normal ACSF, we recorded from 26 non-burst neurons in dTRN slices. In the presence of TTX (0.5 μM), the depolarizing current step did not evoke a transient depolarization in 10 of 26 neurons (Fig. 3*B*, Non-burst). However, in the remaining 16 neurons a small amplitude, transient depolarizing potential was evoked (e.g. see Fig. 4*B*, Small depolarization). This depolarization averaged 4.6 ± 3.1 mV ($n = 16$, range 2–10 mV), and was significantly smaller than a normal LTS evoked in typical burst neurons ($P < 0.01$, Mann–Whitney test). In control conditions, typical burst neurons recorded from vTRN slices produced clear burst discharge (Fig. 3*B*, Typical burst). In TTX (0.5 μM), a stereotypical LTS was evoked in all typical burst neurons with an average amplitude of 24.9 ± 5.8 mV ($n = 16$, Fig. 3*B*, Typical burst). Atypical burst neurons also produced an LTS in the presence of TTX. The LTS amplitude evoked in atypical burst neurons was significantly greater than those in typical burst neurons (Fig. 3*B*, Atypical burst; 30.6 ± 4.3 mV, $n = 16$, $P < 0.05$, Mann–Whitney). In addition, the shape of the LTS differed between typical burst and atypical burst neurons. The duration of the LTS (measured at 50% peak amplitude) in atypical burst neurons averaged 48.2 ± 11.0 ms ($n = 16$) and was significantly greater than typical burst neurons (34.1 ± 11.4 ms, $n = 16$, $P < 0.05$, Mann–Whitney). In these neurons, the atypical burst neurons had significantly higher input resistances (404 ± 130 MΩ; $n = 16$) compared to the typical burst neurons (205 ± 83 MΩ; $P < 0.01$, Mann–Whitney); however, there was not a statistically significant relationship between LTS amplitude and input resistance.

In order to examine if non-burst TRN neurons lack the low threshold, transient calcium current, I_T, membrane currents were recorded. Following conditioning hyperpolarization voltage steps (-50 to -125 mV, 5 mV increments, 1 s duration, Fig. 3*Ca*) a step command to -50 mV was applied to evoke the low threshold transient current, I_T, while not activating high threshold Ca^{2+} currents. In non-burst TRN neurons that produced no LTS in response to current steps in current clamp mode (Fig. 3*B*, Non-burst), the voltage clamp protocol did not produce any transient inward current in 6 of 7 neurons, suggesting a lack of I_T (Fig. 3*Cb*, Non-burst). In the remaining non-burst neuron, a very small

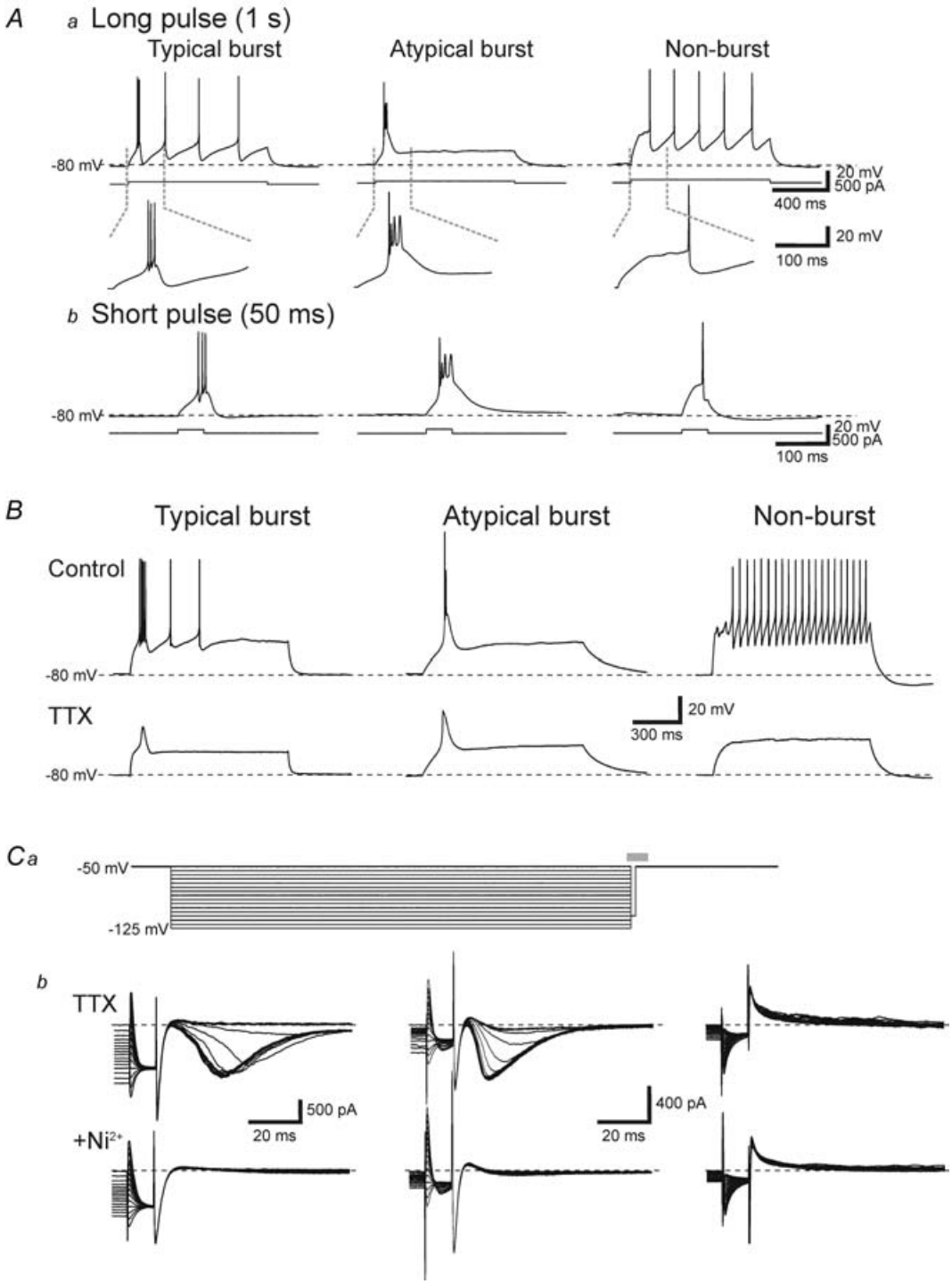

Figure 3. Non-burst TRN neurons lack I_T
A, similar burst discharges are produced by both long- and short-duration current pulses. *a*, long-duration current pulses (1 s duration) evoke characteristic discharges in TRN neuron subtypes similar to that in Fig. 2*Ab*. In the same neurons, a shorter duration current pulse (50 ms duration) evokes a similar discharge as the one second pulse in each subtype of TRN neuron. *B*, following the addition of TTX (0.5 μM), many non-burst neurons (right) lack an LTS or any transient depolarization in response to depolarizing current steps. In contrast, typical burst (left) and atypical burst (middle) neurons produced large amplitude low threshold Ca^{2+} spikes in all neurons tested. The amplitude of the low threshold Ca^{2+} spikes in atypical burst neurons was consistently greater than in typical burst neurons. All neurons were manually hyperpolarized to membrane potentials of −80 mV (dashed line). *Ca*, the

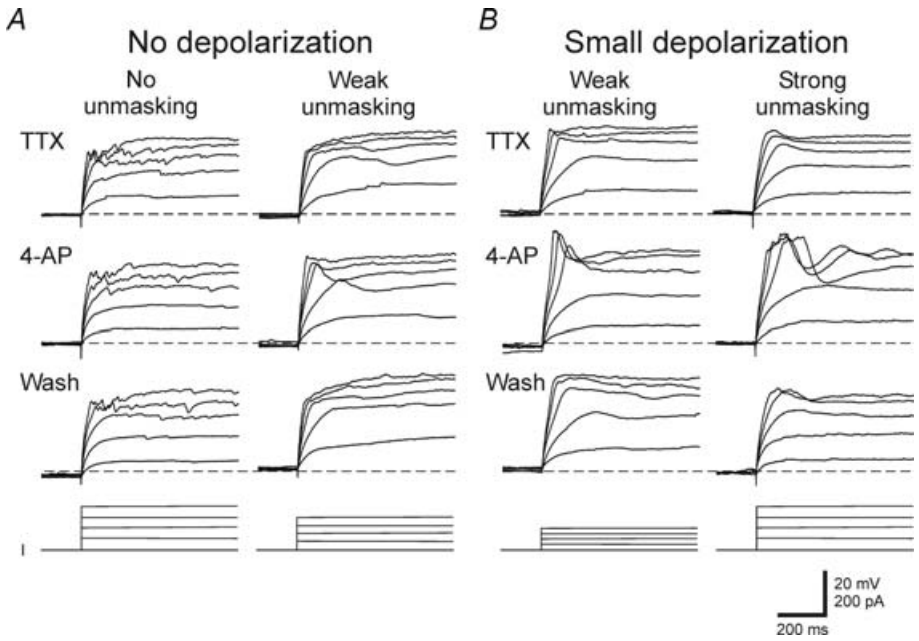

Figure 4. The underlying effect of 4-AP on non-burst neurons
At a holding potential of −80 mV, a depolarizing step current injection in the presence of TTX produced either no depolarizing potential ($n = 6$) or a transient depolarizing potential ($n = 5$) in non-burst neurons ($n = 11$). *A*, in TRN neurons that produced no transient depolarization in TTX, 4-AP (5 mM) produced no unmasking of a transient response in 3 of 6 neurons, but unmasked a small depolarization in the remaining 3 neurons (weak unmasking). *B*, in non-burst neurons that produced small depolarizing potentials in TTX, 4-AP (5 mM) application increased the small depolarization in all 5 neurons in a reversible manner. In 2 of 5 cells, 4-AP application unmasked a normal appearing low threshold Ca^{2+} spike. Dashed line indicates −80 mV. The bottom traces (I) indicate depolarizing current steps.

transient current (−87.3 pA) was evoked. In all typical burst neurons tested, a transient inward current was evoked and the peak amplitude of the current averaged -630 ± 378 pA ($n = 11$; Fig. 3*Cb*, typical burst). The peak inward current evoked in atypical burst neurons did not significantly differ from typical burst neurons (Fig. 3*Cb*, atypical burst; -654 ± 228 pA, $n = 10$, $P > 0.1$, Mann–Whitney test). In order to verify the transient inward current is indeed a Ca^{2+} current, we next tested if the general Ca^{2+} channel blocker Ni^{2+} attenuated the transient inward current. Bath application of Ni^{2+} (1.0–2.0 mM) completely attenuated the transient inward current in all typical and atypical burst neurons tested ($n = 10$, Fig. 3*Cb*).

Considering the similar activation characteristics of the voltage-dependent outward K^+ current, I_A and I_T, previous studies suggest that the lack of burst discharge in dLGN interneurons may result from overlapping activation of these two currents (Pape *et al.* 1994). We next tested if the transient K^+ current, I_A, could mask or prevent an LTS in non-burst TRN neurons. In order to test this, recordings were obtained from 11 non-burst TRN neurons that produced either no transient depolarization ($n = 6$) or a small amplitude transient depolarization (< 5 mV, $n = 5$) in response to depolarizing current steps (1 s, 10–40 pA increments, 15 steps) in TTX (0.5 μM, Fig. 4). The I_A antagonist 4-aminopoyridine (4-AP, 0.05–5 mM) was then bath applied and the subsequent effect on the response to depolarizing current pulses was examined. In six neurons with no transient depolarization, the addition of 4-AP had no effect on the transient depolarizations in three neurons (Fig. 4*A*, No unmasking). In the

voltage protocol to isolate I_T with depolarization to −50 mV from different holding potentials (−50 to −125 mV; 5 mV increments; 1 s duration). *b*, the current traces were obtained in the interval indicated as the grey bar in *a*. In TTX, I_T was not detected in non-burst TRN neurons (6 of 7 neurons tested). However, a typical I_T was evoked in all typical burst neurons tested. The I_T evoked in atypical burst neurons appeared qualitatively similar to those in typical burst neurons. In order to verify that I_T in these neurons are indeed a Ca^{2+}-dependent current, we next tested the sensitivity of the I_T to the Ca^{2+} channel blocker, nickel. Bath application of nickel (1.0–2.0 mM) completely attenuated I_T in all typical and atypical burst neurons tested. In non-burst TRN neurons, nickel produced no changes in current responses.

remaining three neurons, a small depolarizing potential was unmasked in the presence of 4-AP suggesting that there may be a very small Ca^{2+}-dependant current in a subgroup of non-burst TRN neurons (Fig. 4*A*, Weak unmasking). In the remaining five neurons, small transient depolarizations (< 5 mV) were evoked by the depolarizing current steps in the presence of TTX (Fig. 4*B*, Small depolarization). Following the addition of 4-AP, larger amplitude transient depolarizations (range 10–25 mV) were unmasked in all five neurons tested (Fig. 4*B*, Small depolarization). In two of these cells, a nearly normal looking LTS was unmasked in 4-AP (Fig. 4*B*, Strong unmasking). In the other three neurons, a larger transient depolarizing potential was unmasked in 4-AP (Fig. 4*B*, Weak unmasking).

Next, we examined whether the blockade of I_A with 4-AP could transform non-burst neurons into burst neurons because the blockade of I_A with 4-AP unmasks an apparent LTS in a small population of non-burst neurons. Small depolarizing steps (1 s duration, 10–40 pA increments, 15 steps) were applied to non-burst TRN neurons without TTX in order to evoke action potential discharge (Fig. 5, Non-burst). In these experiments the ionotropic glutamate receptors antagonists DNQX (20 μM) and CPP (10 μM) were included in the bath to attenuate 4-AP induced epileptiform discharges. In seven non-burst neurons held at hyperpolarized membrane potentials (-80 mV), the depolarizing current steps only produced tonic action potential discharge (Fig. 5, Non-burst). Following the addition of 4-AP (0.5 mM), these neurons still produced tonic discharge (Fig. 5, Non-burst; 4-AP), suggesting that the unmasked LTS observed in some non-burst neurons is not sufficient to evoke burst firing. We also examined whether blocking I_A in typical burst and atypical burst neurons could affect their burst firing properties. In all five typical burst TRN neurons, the depolarizing current steps produced burst discharge (Fig. 5, Typical burst). Following the addition of 4-AP, the burst discharge of these cells remained. There was a small decrease in the amplitude of the 2nd action potential within the burst (pre: 95.4 ± 7.2 mV, 4-AP: 86.4 ± 8.2 mV, $n = 5$, $P > 0.1$, Wilcoxon matched pairs test) but it was not significantly different as with atypical burst neurons. In a similar manner, the addition of 4-AP did not alter the general features of the atypical burst neuron discharge. In control conditions, in response to a depolarizing current step, the atypical burst neurons produced a discharge consisting of an initial short duration action potential followed by a couple of broader transient depolarizations (Fig. 5, Atypical burst). In 4-AP, the discharge had a similar shape as control conditions; however, the last transient depolarization was longer in duration (Fig. 5, Atypical burst inset, arrow). This latter depolarization was produced in 4 of 5 neurons, and was insensitive to TTX, suggesting this response probably results from activation of a high threshold calcium current, such as an L-current.

Discussion

In the present study, we found that TRN neurons can be easily differentiated into three subtypes based on their firing discharge mode: non-burst, atypical burst and typical burst neurons. These neuronal subtypes also have other distinguishing intrinsic properties such as resting membrane potential and input resistance. TRN neurons have previously been differentiated by their distinct morphology (Scheibel & Scheibel, 1966; Spreafico *et al.* 1988; Avanzini *et al.* 1989; Spreafico *et al.* 1991); however, the differences in intrinsic properties that we observed were not associated with distinct morphologies. Perhaps the most intriguing feature of these TRN neuron subtypes is that they are differentially distributed within TRN. Non-burst and atypical burst neurons were predominantly located within the dorsal TRN, whereas typical burst neurons were predominantly localized to

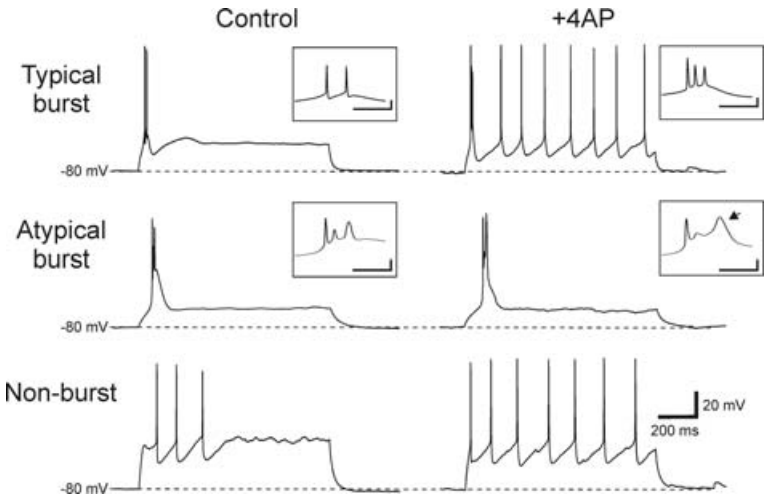

Figure 5. Blocking I_A does not alter action potential discharge properties of non-burst and typical burst TRN neurons
Typical burst: in this neuron, the depolarizing current step produces clear burst discharge ring atop an LTS. In the presence of 4-AP (0.5 mM), the burst discharge persists. Atypical burst: in this neuron, the depolarizing current step produces the atypical burst discharge consisting of an initial sharp action potential followed by broader transient depolarizations (see inset). In 4-AP, a similar discharge pattern is observed; however, the last transient depolarization (arrow in inset) has a longer duration. Non-burst: from a membrane potential of -80 mV, depolarizing current steps in control solution produced no burst discharge in this neuron. In the presence of 4-AP, the depolarizing current step still produces only tonic discharge with a shorter latency to the first action potential. Inset scale: 20 mV, 20 ms.

the ventral TRN region. These two novel TRN neuron subtypes, non-burst and atypical burst neurons, were present at all ages tested (postnatal ages: 10–28 days) indicating that the lack of burst firing is not age dependent in the range tested. The absence of burst discharge in non-burst neurons results from the lack or minimal amount of I_T in these cells as indicated from the present data. Burst discharge of TRN neurons has long been considered a ubiquitous characteristic of TRN neurons as well as an important component contributing to intrathalamic rhythmic activities associated with different levels of arousal and certain pathophysiological conditions such as absence epilepsy (Glenn & Steriade, 1982; Jahnsen & Llinás, 1984*a*; Coulter *et al.* 1989; Steriade *et al.* 1993; von Krosigk *et al.* 1993). The functional significance of these different distinct firing patterns among TRN neuronal subtypes (non-burst, atypical burst) to intrathalamic rhythmic activities as well as overall function of thalamocortical circuits remains unclear. Interestingly, the non-burst neurons were localized in the dTRN, a region predominantly associated with the visual system and thus may serve a unique role for visual processing (Jones, 1975; Hale *et al.* 1982; French *et al.* 1985; Shosaku *et al.* 1989; Pinault *et al.* 1995*a*; Coleman & Mitrofanis, 1996).

Ubiquitous burst discharge of TRN neurons?

Burst discharge has been considered a ubiquitous feature of virtually all thalamic neurons including TRN neurons. Almost all studies involving TRN and perigeniculate nucleus (PGN, analogous to visual TRN in higher animals such as ferrets, cats, monkeys and humans) indicate that these neurons can produce a transient, high frequency action potential discharge (Sefton & Burke, 1966; Sumitomo *et al.* 1976; Dubin & Cleland, 1977; Hale *et al.* 1982; Kayama *et al.* 1982; Kayama *et al.* 1986; Steriade & Llinás, 1988; Amzica *et al.* 1992). The burst discharge of TRN neurons results from activation of the voltage-dependent, low threshold, transient calcium current, I_T, which in turn produces a transient depolarization on top of which a high frequency discharge of sodium-dependent action potentials can occur (Ahlsén & Lindström, 1982; Steriade & Llinás, 1988; Amzica *et al.* 1992; Huguenard & Prince, 1992; von Krosigk *et al.* 1993; Bal *et al.* 1995). To date, there are two reports in the literature indicating a lack of burst discharge in TRN neurons, one *in vivo* and one *in vitro* study: however, these neurons were a small fraction of the population, and thus the localization and morphology of these neurons were not systematically studied (Contreras *et al.* 1992; Brunton & Charpak, 1997). Furthermore, the cellular mechanisms underlying the lack of burst discharge were not examined.

In the present study, we found two distinct types of TRN neurons that do not produce stereotypical burst output: non-burst and atypical burst neurons. Following blockade of action potentials with TTX, atypical burst neurons appear to produce a voltage-dependent LTS in response to a depolarizing current step with larger amplitude and longer duration than that in typical burst neurons. In addition, the burst discharge of atypical burst neurons differs in that the action potentials riding atop the LTS have lower amplitude and longer duration than the initial normal-appearing action potential (e.g. see Fig. 2). The decreased amplitude of the apparent action potentials may result from Na^+ channel inactivation considering the significantly greater input resistance of atypical burst neurons compared to typical burst neurons.

In contrast, non-burst neurons appear to be a mixed population of neurons regarding the presence of a low threshold calcium current. In control conditions, these cells only produce tonic discharge, and no burst discharge. In the presence of TTX, and from a hyperpolarized membrane potential, approximately half of the neurons produce no transient depolarizations in response to depolarizing current step injections, suggesting the lack of I_T. In the remaining neurons, there is a small amplitude, transient depolarization reminiscent of a truncated I_T, but obviously insufficient to produce burst discharge. If we then add the K^+-channel blocker 4-AP to non-burst neurons that have a small transient depolarization, we unmask a larger amplitude transient depolarization that resembles an LTS. Thus, it appears that a subpopulation of non-burst TRN neurons do indeed have some I_T, but as a result of overlapping activation characteristics of the voltage-dependent, transient K^+ current, I_A and I_T, activation of I_A occludes the transient LTS needed for burst discharge; however, the unmasked LTS in these non-burst neurons is not sufficient to evoke burst firing (Fig. 5, Non-burst). The functional role of this smaller transient depolarization may be to modulate integration of afferent synaptic input, and thus in certain conditions in which I_A may be modulated or attenuated, afferent information processing could be influenced by I_T.

Functional significance of the heterogeneous TRN neuron subtypes

The functional role of these different TRN neuronal subtypes remains unclear. Perhaps the best insight may be due to the non-uniform distribution of these different neuronal subtypes. Non-burst and atypical burst neurons are preferentially localized within the dorsal TRN, whereas the typical burst neurons are primarily located in the ventral TRN. The TRN can be subdivided into different modality specific regions and the dorsal TRN is primarily associated with visual information processing (Jones, 1975; Crabtree & Killackey, 1989; Pinault *et al.* 1995*a*; Coleman & Mitrofanis, 1996). In rodents, the dorsal TRN primarily innervates the dLGN and the higher order

visual thalamic nucleus, the lateral posterior nucleus, both structures that are related to visual processing (Coleman & Mitrofanis, 1996). It will be of considerable interest to determine if these multiple TRN subtypes are localized within the visual regions of TRN in other species.

Interestingly, various studies have investigated the prevalence of burst discharge during different levels of arousal. It is generally accepted that during periods of drowsiness, slow-wave sleep, and certain pathophysiological conditions, the intrathalamic circuit can produce rhythmic activities that are dependent on burst output of TRN and associated thalamocortical relay neurons. Neuromodulators that have been shown to decrease the burst output of either neuronal population also attenuate the rhythmic activity. Furthermore, burst discharge of thalamocortical neurons has also been observed in the wake animal as well, but to a much lesser extent (Guido & Weyand, 1995; Ramcharan *et al.* 2000; Edeline *et al.* 2000; Fanselow *et al.* 2001; Massaux *et al.* 2004). A critical component of thalamocortical burst discharge is a preburst hyperpolarization of the thalamocortical neuron, which is typically thought to be in response to a strong inhibition produced by TRN neurons, possibly burst discharge of these TRN cells. From various *in vivo* studies, it appears that burst frequency in LGN neurons is significantly less than that observed in other sensory modalities including both somatosensory and auditory systems (Guido & Weyand, 1995; Edeline *et al.* 2000; Ramcharan *et al.* 2000; Fanselow *et al.* 2001; Weyand *et al.* 2001; Massaux *et al.* 2004; Ramcharan *et al.* 2005). Perhaps this decreased frequency is a direct result of the significantly decreased numbers of TRN neurons that can produce burst discharge that innervate the dLGN as suggested by this study.

Another important issue regarding these different neuronal subtypes is the actual inhibitory influence on the postsynaptic neurons. In paired recordings of synaptically coupled PGN and LGN relay neurons, tonic discharge of the PGN neuron activates short-lasting $GABA_A$ receptor mediated activity in the thalamocortical neuron, whereas burst discharge of the PGN neuron produces a longer-lasting hyperpolarization via activation of $GABA_B$ receptors (Kim *et al.* 1997). While the firing properties of the cell clearly influence the postsynaptic neuron, the actual axonal arborization and number of synaptic contacts can also significantly influence the coupling strength between the presynaptic and postsynaptic neuron. In the rodent somatosensory thalamus, TRN neurons can give rise to a variety of axonal arbors ranging from very focal, high density of putative release sites to very widespread, low density arbors (Scheibel & Scheibel, 1966; Yen *et al.* 1985; Pinault *et al.* 1995*b*; Cox *et al.* 1996). From paired recordings in the somatosensory region, the strength of postsynaptic inhibition is positively correlated with the density of the axonal arbor (Cox *et al.* 1997*a*). It will be interesting to determine how the different TRN subtypes influence the postsynaptic neuron. Do the different firing characteristics described here give rise to distinct postsynaptic outputs? Secondly, do the axonal arbors of these distinct TRN subtypes differ as well? Reconstruction of the axonal arbors will be required to address the latter issue. Of particular interest would be the atypical burst neurons. Clearly, the amplitude and duration of action potentials in these neurons differ significantly from typical burst neurons, but does this translate to a difference in the axonal output of these cells? Furthermore, it will be important to examine whether non-burst neurons provide weak inhibitory influences onto relay neurons, or perhaps because they lack the bursting mode, these cells respond to afferent synaptic transmission in a more linear manner than cells that can burst.

Our study clearly indicates electrophysiological heterogeneity amongst TRN neurons that is related to their dorsal/ventral location within the TRN. Considering that discrete regions of TRN have been associated with specific sensory modalities (Jones, 1975), we speculate that each sensory sector of the TRN may consist of multiple TRN subtypes. The functional role of these different TRN subtypes on thalamocortical information processing remains open-ended for future investigation.

References

Ahlsén G & Lindström S (1982). Excitation of perigeniculate neurones via axon collaterals of principal cells. *Brain Res* **236**, 477–481.

Ahlsén G, Lindström S & Lo F-S (1985). Interaction between inhibitory pathways to principal cells in the lateral geniculate nucleus of the cat. *Exp Brain Res* **58**, 134–143.

Amzica F, Nuñez A & Steriade M (1992). Delta frequency (1–4 Hz) oscillations of perigeniculate thalamic neurons and their modulation by light. *Neurosci* **51**, 285–294.

Avanzini G, De Curtis M, Panzica F & Spreafico R (1989). Intrinsic properties of nucleus reticularis thalami neurones of the rat studied in vitro. *J Physiol* **416**, 111–122.

Bal T, von Krosigk M & McCormick DA (1995). Role of the ferret perigeniculate nucleus in the generation of synchronized oscillations in vitro. *J Physiol* **483**, 665–685.

Bourassa J, Pinault D & Deschênes M (1995). Corticothalamic projections from the cortical barrel field to the somatosensory thalamus in rats: a single-fibre study using biocytin as an anterograde tracer. *Eur J Neurosci* **7**, 19–30.

Brunton J & Charpak S (1997). Heterogeneity of cell firing properties and opioid sensitivity in the thalamic reticular nucleus. *Neuroscience* **78**, 303–307.

Coleman KA & Mitrofanis J (1996). Organization of the visual reticular thalamic nucleus of the rat. *Eur J Neurosci* **8**, 388–404.

Conley M & Diamond IT (1990). Organization of the visual sector of the thalamic reticular nucleus in galago. *Eur J Neurosci* **2**, 211–226.

Contreras D, Curró Dossi R & Steriade M (1992). Bursting and tonic discharges in two classes of reticular thalamic neurons. *J Neurophysiol* **68**, 973–977.

Contreras D, Curró Dossi R & Steriade M (1993). Electrophysiological properties of cat reticular thalamic neurones in vivo. *J Physiol* **470**, 273–294.

Coulter DA, Huguenard JR & Prince DA (1989). Calcium currents in rat thalamocortical relay neurones: kinetic properties of the transient, low-threshold current. *J Physiol* **414**, 587–604.

Cox CL, Huguenard JR & Prince DA (1996). Hetereogenous axonal arborizations of rat thalamic reticular neurons in the ventrobasal nucleus. *J Comp Neurol* **366**, 416–430.

Cox CL, Huguenard JR & Prince DA (1997*a*). Nucleus reticularis neurons mediate diverse inhibitory effects in thalamus. *Proc Natl Acad Sci U S A* **94**, 8854–8859.

Cox CL, Huguenard JR & Prince DA (1997*b*). Peptidergic modulation of intrathalamic circuit activity in vitro: Actions of cholecystokinin. *J Neurosci* **17**, 70–82.

Crabtree JW (1992). The somatopic organization within the cat's thalamic reticular nucleus. *Eur J Neurosci* **4**, 1352–1361.

Crabtree JW (1996). Organization in the somatosensory sector of the cat's thalamic reticular nucleus. *J Comp Neurol* **366**, 207–222.

Crabtree JW (1999). Intrathalamic sensory connections mediated by the thalamic reticular nucleus. *Cellular Mol Life Sci* **56**, 683–700.

Crabtree JW, Collingridge GL & Isaac JTR (1998). A new intrathalamic pathway linking modality-related nuclei in the dorsal thalamus. *Nat Neurosci* **1**, 389–394.

Crabtree JW & Isaac JT (2002). New intrathalamic pathways allowing modality-related and cross-modality switching in the dorsal thalamus. *J Neurosci* **22**, 8754–8761.

Crabtree JW & Killackey HP (1989). The topographic organization and axis of projection within the visual sector of the rabbit's thalamic reticular nucleus. *Eur J Neurosci* **1**, 94–109.

Deschênes M, Roy JP & Steriade M (1982). Thalamic bursting mechanism: an inward slow current revealed by membrane hyperpolarization. *Brain Res* **239**, 289–293.

Domich L, Oakson G & Steriade M (1986). Thalamic burst patterns in the naturally sleeping cat: a comparison between cortically-projecting and reticularis neurones. *J Physiol* **379**, 429–449.

Dubin MW & Cleland BG (1977). Organization of visual inputs to interneurons of lateral geniculate nucleus of the cat. *J Neurophysiol* **40**, 410–427.

Edeline JM, Manunta Y & Hennevin E (2000). Auditory thalamus neurons during sleep: changes in frequency selectivity, threshold, and receptive field size. *J Neurophysiol* **84**, 934–952.

Fanselow EE, Sameshima K, Baccala LA & Nicolelis MA (2001). Thalamic bursting in rats during different awake behavioral states. *Proc Natl Acad Sci U S A* **98**, 15330–15335.

French CR, Sefton AJ & Mackay-Sim A (1985). The inhibitory role of the visually responsive region of the thalamic reticular nucleus in the rat. *Exp Brain Res* **57**, 471–479.

Glenn LL & Steriade M (1982). Discharge rate and excitability of cortically projecting intralaminar thalamic neurons during waking and sleep states. *J Neurosci* **2**, 1387–1404.

Govindaiah G & Cox CL (2004). Synaptic activation of metabotropic glutamate receptors regulates dendritic outputs of thalamic interneurons. *Neuron* **41**, 611–623.

Guido W & Weyand T (1995). Burst responses in thalamic relay cells of the awake behaving cat. *J Neurophysiol* **74**, 1782–1786.

Hale PT, Sefton AJ, Baur LA & Cottee LJ (1982). Interrelations of the rat's thalamic reticular and dorsal lateral geniculate nuclei. *Exp Brain Res* **45**, 217–229.

Horikawa K & Armstrong WE (1988). A versatile means of intracellular labeling: injection of biocytin and its detection with avidin conjugates. *J Neurosci Methods* **25**, 1–11.

Houser CR, Vaughn JE, Barber RP & Roberts E (1980). GABA neurons are the major cell type of the nucleus reticularis thalami. *Brain Res* **200**, 341–354.

Huguenard JR & Prince DA (1992). A novel T-type current underlies prolonged Ca^{2+}-dependent burst firing in GABAergic neurons of rat thalamic reticular nucleus. *J Neurosci* **12**, 3804–3817.

Huguenard JR & Prince DA (1994). Intrathalamic rhythmicity studies in vitro: Nominal t-current modulation causes robust antioscillatory effects. *J Neurosci* **14**, 5485–5502.

Jahnsen H & Llinás R (1984*a*). Electrophysiological properties of guinea-pig thalamic neurones: an in vitro study. *J Physiol* **349**, 205–226.

Jahnsen H & Llinás R (1984*b*). Ionic basis for the electroresponsiveness and oscillatory properties of guinea-pig thalamic neurones in vitro. *J Physiol* **349**, 227–247.

Jones EG (1975). Some aspects of the organization of the thalamic reticular complex. *J Comp Neurol* **162**, 285–308.

Kayama Y, Negi T, Sugitani M & Iwama K (1982). Effects of locus coeruleus stimulation on neuronal activities of dorsal lateral geniculate nucleus and perigeniculate reticular nucleus of the rat. *Neuroscience* **7**, 655–666.

Kayama Y, Sumitomo I & Ogawa T (1986). Does the ascending cholinergic projection inhibit or excite neurons in the rat thalamic reticular nucleus. *J Neurophysiol* **56**, 1310–1320.

Kim U, Sanchez-Vives MV & McCormick DA (1997). Functional dynamics of GABAergic inhibition in the thalamus. *Science* **278**, 130–134.

Lee SH & Cox CL (2003). Vasoactive intestinal peptide selectively depolarizes thalamic relay neurons and attenuates intrathalamic rhythmic activity. *J Neurophysiol* **90**, 1224–1234.

Lee SH & Cox CL (2006). Excitatory actions of vasoactive intestinal peptide on mouse thalamocortical neurons are mediated by VPAC2 receptors. *J Neurophysiol* **96**, 858–871.

Lee SM, Friedberg MH & Ebner FF (1994). The role of GABA-mediated inhibition in the rat ventral posterior medial thalamus. I. Assessment of receptive field changes following thalamic reticular nucleus lesions. *J Neurophysiol* **71**, 1702–1715.

Lee SH, Govindaiah G & Cox CL (2004). Is burst firing a ubiquitous characteristic of thalamic reticular neurons? *Soc Neurosci Abstr* **30**, 983.14.

Lisman JE (1997). Bursts as a unit of neural information: making unreliable synapses reliable. *Trends Neurosci* **20**, 38–43.

Massaux A, Dutrieux G, Cotillon-Williams N, Manunta Y & Edeline JM (2004). Auditory thalamus bursts in anesthetized and non-anesthetized states: contribution to functional properties. *J Neurophysiol* **91**, 2117–2134.

Mulle C, Madariaga A & Deschênes M (1986). Morphology and electrophysiological properties of reticularis thalami neurons in cat: In vivo study of a thalamic pacemaker. *J Neurosci* **6**, 2134–2145.

Pape H-C, Budde T, Mager R & Kisvárday ZF (1994). Prevention of Ca^{2+}-mediated action potentials in GABAergic local circuit neurones of rat thalamus by a transient K^+ current. *J Physiol* **478**, 403–422.

Paxinos G & Watson C (1986). *The Rat Brain in Stereotaxic Coordinates*. Academic Press, Orlando.

Pinault D, Bourassa J & Deschênes M (1995*a*). Thalamic reticular input to the rat visual thalamus: a single fiber study using biocytin as an anterograde tracer. *Brain Res* **670**, 147–152.

Pinault D, Bourassa J & Deschênes M (1995*b*). The axonal arborization of single thalamic reticular neurons in the somatosensory thalamus of the rat. *Eur J Neurosci* **7**, 31–40.

Ramcharan EJ, Gnadt JW & Sherman SM (2000). Burst and tonic firing in thalamic cells of unanesthetized, behaving monkeys. *Vis Neurosci* **17**, 55–62.

Ramcharan EJ, Gnadt JW & Sherman SM (2005). Higher-order thalamic relays burst more than first-order relays. *Proc Natl Acad Sci U S A* **102**, 12236–12241.

Scheibel ME & Scheibel AB (1966). The organization of the nucleus reticularis thalami: a golgi study. *Brain Res* **1**, 43–62.

Sefton AJ & Burke W (1966). Mechanism of recurrent inhibition in the lateral geniculate nucleus of the rat. *Nature* **211**, 1276–1278.

Sherman SM & Guillery RW (2002). The role of the thalamus in the flow of information to the cortex. *Philos Trans R Soc Lond B Biol Sci* **357**, 1695–1708.

Shosaku A, Kayama Y, Sumitomo I, Sugitani M & Iwama K (1989). Analysis of recurrent inhibitory circuit in rat thalamus: Neurophysiology of the thalamic reticular nucleus. *Prog Neurobiol* **32**, 77–102.

Spreafico R, Battaglia G & Frassoni C (1991). The reticular thalamic nucleus (RTN) of the rat: cytoarchitectural, golgi, immunocytochemical, and horseradish peroxidase study. *J Comp Neurol* **304**, 478–490.

Spreafico R, DeCurtis M, Frassoni C & Avanzini G (1988). Electrophysiological characteristics of morphologically identified reticular thalamic neruons from rat slices. *Neurosci* **27**, 629–638.

Steriade M, Domich L & Oakson G (1986). Reticularis thalami neurons revisited: activity changes during shifts in states of vigilance. *J Neurosci* **6**, 68–81.

Steriade M & Llinás R (1988). The functional states of the thalamus and the associated neuronal interplay. *Physiol Rev* **68**, 649–742.

Steriade M, McCormick DA & Sejnowski TJ (1993). Thalamocortical oscillations in the sleeping and aroused brain. *Science* **262**, 679–685.

Sumitomo I, Nakamura M & Iwama K (1976). Location and function of the so-called interneurons of rat lateral geniculate body. *Exp Neurol* **51**, 110–123.

von Krosigk M, Bal T & McCormick DA (1993). Cellular mechanisms of a synchronized oscillation in the thalamus. *Science* **261**, 361–364.

Warren RA, Agmon A & Jones EG (1994). Oscillatory synaptic interactions between ventroposterior and reticular neurons in mouse thalamus in vitro. *J Neurophysiol* **72**, 1993–2003.

Weyand TG, Boudreaux M & Guido W (2001). Burst and tonic response modes in thalamic neurons during sleep and wakefulness. *J Neurophysiol* **85**, 1107–1118.

Yen CT, Conley M, Hendry SHC & Jones EG (1985). The morphology of physiologically identified GABAergic neurons in the somatic sensory part of the thalamic reticular nucleus in the cat. *J Neurosci* **5**, 2254–2268.

Acknowledgements

This research was supported by the National Institutes of Health (EY014024).